



Title	Identification, cDNA cloning, and expression analysis of dermatopontin in the goldfish <i>Carassius auratus</i>
Author(s)	Komatsu, Norihiko; Ogawa, Nobuhiro; Iimura, Kurin; Ura, Kazuhiro; Takagi, Yasuaki
Citation	Fisheries science, 80(6), 1249-1256 https://doi.org/10.1007/s12562-014-0814-y
Issue Date	2014-11
Doc URL	http://hdl.handle.net/2115/60034
Rights	The final publication is available at www.springerlink.com
Type	article (author version)
File Information	Komatsu et al Revised text-3.pdf



[Instructions for use](#)

1 **Identification, cDNA cloning, and expression analysis of dermatopontin in the goldfish *Carassius auratus***

2

3 **Norihiko Komatsu • Nobuhiro Ogawa • Kurin Iimura • Kazuhiro Ura • Yasuaki Takagi**

4

5 Graduate School of Fisheries Sciences, Hokkaido University, Minato-cho 3-1-1, Hakodate, Hokkaido 041-8611,

6 Japan

7

8 *Present address:* Nobuhiko Komatsu, Saku Branch, Nagano Prefectural Fisheries Experimental Station,

9 Takayagi 282, Saku, Nagano 385-0042, Japan

10 *Present address:* Nobuhiro Ogawa, Atmosphere and Ocean Research Institute, The University of Tokyo, 5-1-5,

11 Kashiwanoha, Kashiwa, Chiba 277-8564, Japan

12 *Present address:* Kurin Iimura, Department of Applied Biological Chemistry, Graduate School of Agricultural

13 and Life Sciences, The University of Tokyo, Yayoi 1-1-1, Bunkyo, Tokyo 113-8657, Japan

14

15 Corresponding author: Yasuaki Takagi

16 Tel/Fax: +81 138 40 5550

17 E-mail: takagi@fish.hokudai.ac.jp

18 E-mail addresses

19 N. Komatsu: komatsu-norihiko-r@pref.nagano.lg.jp

20 N. Ogawa: n-ogawa@aori.u-tokyo.ac.jp

21 K. Iimura: akurin@mail.ecc.u-tokyo.ac.jp

22 K. Ura: kazu@fish.hokudai.ac.jp

23 Y. Takagi: takagi@fish.hokudai.ac.jp

24

25

26 **Abstract**

27

28 Fish collagen is a potential source of a scaffold for cells during tissue engineering, because it has low risk of
29 zoonosis. Since the collagen fibril assembly has a significant impact on the functionality of the scaffold, the
30 ability to replicate the fibril assembly of human tissues is critical. As a first step in determining the mechanism
31 of fish collagen fibril assembly, we identified non-collagenous proteins (NCPs), the potential regulators of fibril
32 assembly *in vivo*. We applied tandem mass spectrometry to analyze NCPs contained in the basal plate of goldfish
33 *Carassius auratus* scales, a collagenous plate having a cornea-like, plywood-like assembly of collagen fibrils.
34 We identified a 19-kDa acidic protein as dermatopontin, the NCP that is a possible regulator of fibril assembly in
35 the mammalian cornea. We cloned a goldfish dermatopontin cDNA of 1074 bp containing an open reading frame
36 encoding 196 amino acids. RT-PCR revealed that dermatopontin mRNA was expressed in a wide range of
37 tissues, including scale, skin, fin, eye, and skeletal muscle. *In situ* hybridization revealed that dermatopontin
38 mRNA was expressed primarily in the basal-plate producing hyposquamal scleroblasts in the scale, suggesting
39 that the dermatopontin is linked to the construction of fibril assembly of the basal-plate collagen.

40

41 **Key words:** biglycan, collagen assembly, dermatopontin, lysyl oxidase, MS/MS analysis, scale, teleost

42

43 **Introduction**

44

45 The exploitation of seafood by-products is an important component of improving the sustainability of the
46 seafood industry. Our research is currently focused on the fabrication of a cellular scaffold for tissue engineering
47 using fish type I collagen [1], which can be extracted from fish offal (e.g., skin, scales, and fins).

48 Collagen is the primary component of the extracellular matrix (ECM) in an animal's body and
49 functions not only as a structural support for tissues, but also as an adhesive substrate for cells and a fundamental
50 regulator of cellular growth and differentiation [2-5]. Because of these properties, collagen has been widely used
51 as a scaffold to support cellular growth and differentiation in both research and tissue engineering [6]. To date,
52 the primary source of medical collagen has been domestic animals (pig and cattle). Recently, however, fish
53 collagen has attracted increased attention [7] as it has a low risk of contamination with diseases that are
54 infectious to human beings, such as bovine spongiform encephalopathy. Additionally, the use of fish collagen
55 raises fewer religious objections than animal collagen.

56 Collagen-based scaffolds having a three-dimensional assembly of collagen fibrils replicating the
57 structure in human tissues are generally believed to have improved functionality for tissue engineering
58 applications. This is because the tissue function in humans is dependent on the tissue-specific three-dimensional
59 assembly of collagen fibrils. In the corneal stroma, for example, multiple layers of type I collagen fibrils are
60 stacked, and the fibrils in one layer are aligned in parallel, whereas those in different layers are aligned
61 perpendicular, resulting in a plywood-like structure [8]. This structure gives tensile strength as well as
62 transparency to the tissue. Thus, to fabricate a functional cornea substitute using collagen, researchers must
63 replicate this complicated collagen fibril assembly. Because of the difficulty associated with artificial regulation
64 of collagen fibril assembly using industrial techniques, technology derived from cellular mechanisms
65 (bioinspired technology) is gaining increased attention [1].

66 Previous studies have revealed that non-collagenous proteins (NCPs) secreted from ECM-producing
67 cells have an important role in the regulation of collagen fibril assembly in animal tissues. For example,
68 knock-out of dermatopontin, one of the NCPs contained in the corneal stroma of mammals, results in larger
69 collagen-fibril spacing (fewer collagen fibrils per unit area of the section) and disrupted fibrillar organization in
70 the cornea [9]. However, the mechanisms controlling fish collagen fibril assembly are poorly understood, and
71 there has been no documentation of NCPs associated with collagen fibril structure to date.

72 The basal plate of teleost fish scales represents an interesting model to study the cellular mechanisms
73 of three-dimensional assembly of fish collagen fibrils. The basal plate is formed of type I collagen fibrils having
74 a cornea-like plywood-like assembly [1]. Our objective was to isolate and identify NCPs from the scale basal
75 plates of the goldfish *Carassius auratus*. We acid-extracted the ECM of the scale basal plate and conducted
76 time-of-flight tandem mass spectrometry (MS/MS). Additionally, we performed cDNA cloning and mRNA
77 expression analysis by RT-PCR and *in situ* hybridization of goldfish dermatopontin, one of the NCPs identified
78 during MS/MS analysis.

79

80 **Materials and methods**

81

82 **Fish and rearing**

83

84 Goldfish (ca. 15 cm fork length) were purchased from a commercial dealer. The animals were held in aerated tap
85 water at 25°C and fed a commercial diet (4C; Nippon Formula Feed Mfg. Co., Ltd., Yokohama, Japan).

86

87 **Protein extraction from scale basal plates**

88

89 After deeply anesthetizing the fish in a 0.1% solution of 2-phenoxyethanol, a total of approximately 700 scales
90 were removed with forceps from five fish. Lateral-line scales were not included. The scales were then washed
91 overnight in multiple cold (4°C) distilled water baths (with stirring) to remove cellular debris. Then, the basal
92 plates were removed using forceps and a scalpel. The wet weight of the pooled basal plates was recorded to two
93 decimal places.

94 To obtain NCPs, we extracted the basal plate with 10 volumes (v/w) of 0.5 M acetic acid under gentle
95 rotation at 4°C for 1 day. Acetic acid is commonly used to extract native collagen molecules from tissues.

96 Therefore, we assumed that the collagen molecules with associated NCPs were extracted by this method.

97 Following extraction, the samples were centrifuged at 2,000xg for 10 min at 4°C, and both the supernatant and
98 precipitate were collected. The supernatant was further centrifuged at 21,500xg for 10 min at 4°C and stored on

99 ice. The precipitate from the first centrifugation was re-extracted as described above, centrifuged twice, and the

100 final supernatant was mixed with the original supernatant and stored on ice. The protein content of the mixed

101 supernatant was quantified using a Micro BCA™ Protein Assay Kit (PIERCE, Rockford, IL, USA).

102

103 Two-dimensional gel electrophoresis

104

105 To characterize the protein profile of the supernatant, we performed two-dimensional gel electrophoresis (2-DE)
106 using the Ettan IPGphor 3 IEF System (GE Healthcare Biosciences, Buckinghamshire, UK) for isoelectric
107 electrophoresis (pI range 3–10) and a slab electrophoresis chamber (Atto, Tokyo, Japan) for SDS-PAGE (15%
108 separating gel). A total of 600 µg of proteins were separated according to the manufacturers' protocols. The
109 separated proteins were detected by silver staining.

110

111 Identification of proteins by tandem mass spectrometry

112

113 To perform mass spectrometry, the protein spots separated by 2-DE were excised and processed according to the
114 manufacturer's protocol (Applied Biosystems, Tokyo, Japan), with a slight modification: a trypsin enhancer
115 (Promega, Madison, WI, USA) was added to enhance trypsin digestion of the sample. The digested peptides
116 were purified using a ZipTip (Millipore, Billerica, MA, USA) and applied to MS/MS (MALDI-TOF-TOF,
117 Applied Biosystems 4700). The tryptic peptide mass fingerprinting and subsequently obtained MS/MS spectra
118 were used for a Mascot search [10] in the Actinopterygii protein database. Proteins were judged to be identified
119 when the amino acid sequences of at least two peptides were significantly ($P < 0.05$) matched with those in the
120 database.

121

122 cDNA cloning of goldfish dermatopontin

123

124 Goldfish were anesthetized in a 0.1% 2-phenoxyethanol solution, and 30 scales were removed from the left flank.
125 The lateral line scales were not used. Total RNA was isolated from the scales using ISOGEN (Nippon gene,
126 Tokyo, Japan) and a FastPure™ RNA kit (Takara, Otsu, Japan). After DNase I (Takara) treatment, first-strand
127 cDNA from 500 µg of total RNA was synthesized using a PrimeScript™ RT reagent kit (Perfect Real Time:
128 Takara). First-strand cDNA was synthesized from 500 µg of total RNA by 5' and 3' RACE using a SMART™
129 RACE cDNA amplification kit (Clontech, Palo Alto, CA, USA).

130

131 To obtain the goldfish dermatopontin fragment, PCR was first performed using the primers
5'-ccccgctctgttgatcatcccaccagc-3' (forward) and 5'-gccctatagtgagtcgtattag-3' (reverse), which were designed

132 based on zebrafish *Danio rerio* sequence data (GenBank accession no. NM_001030085). After determining the
133 partial sequences, 3' RACE was performed using the gene-specific primer 5'-aactggaagaattcgcggcc-3' and
134 adopter primer 5'-aactggaagaattcgcggcc-3'. Following the first 3' RACE PCR, a nested PCR was performed
135 using the gene-specific primer 5'-tcgcgccgcaggaa-3' and adopter primer 5'-tcgcgccgcaggaa-3'. Then, 5' RACE
136 was performed using the mixed adopter primers 5'-ctaatacactcactatagggcaagcagtggtat-3' and
137 5'-ctaatacactcactatagggc-3' and the gene-specific primer 5'-gccctatagtgagtcgtattag-3'.

138 The amplified cDNAs were ligated into a pGEM-T Easy vector (Promega, Madison, WI, USA), and
139 XL-1 Blue was transformed. Nucleotide sequences were analyzed with a Big-Dye Terminator v3.1 Cycle
140 Sequencing kit using an ABI PRISM 3130xl Genetic Analyzer (Applied Biosystems, Tokyo, Japan).
141 Multiple amino acid sequence alignments were produced with the ClustalW2 program
142 (<http://www.ebi.ac.uk/Tools/clustalw2/index.html>).

143

144 Expression analyses of goldfish dermatopontin mRNA

145

146 The tissue distribution of dermatopontin mRNA expression was examined using RT-PCR. Goldfish were deeply
147 anesthetized using a 0.1% 2-phenoxyethanol solution, and then decapitated. Each animal was dissected and brain,
148 caudal fin, eye, heart, kidney, liver, scales, skeletal muscle, skin (without scales), swim bladder, and blood cells
149 were collected. Each scale was cut in half with scissors, and the anterior half (lacking epithelial tissue) was used
150 in subsequent analyses. Total RNA was extracted using ISOGEN and a FastPure™ RNA kit. After DNase I
151 (Takara) treatment, first strand cDNA from 91.5–100 µg of total RNA was synthesized using a PrimeScript™
152 RT reagent Kit (Perfect Real Time). The primers for PCR, 5'-gacttcaggatgagctcagca-3' (forward) and
153 5'-accafcaacaagcccattg-3' (reverse), were designed based on the cDNA data obtained in this study. GAPDH was
154 used as an internal standard. The primers for GAPDH, 5'-caagccatctctgtgtccag-3' (forward) and
155 5'-accagttgaagcaggatga-3' (reverse), were designed from sequence data in GenBank (GenBank accession no.
156 AY641443).

157 *In situ* hybridization was conducted to localize dermatopontin mRNA expression in the scale. A 504
158 bp fragment (nt 488-991) of dermatopontin cDNA was amplified by PCR using the primers
159 5'-ccagttacggctactcataa-3' (forward) and 5'-gtctgttactccatctgag-3' (reverse), and ligated into a pGEM-T Easy
160 vector (Promega). The PCR product in the pGEM-T Easy vector was further amplified with M 13 primers and

161 used as a template to synthesize digoxigenin-labeled probes with T7 and SP6 RNA polymerase (Roche,
162 Mannheim, Germany).

163 The scale forming cells (scleroblasts) of the ontogenetic scales in goldfish, and particularly the
164 basal-plate producing hyposquamal scleroblasts, are flat and small [11]. Because of this, we predicted that the
165 hybridization signal would be difficult to detect. To improve the likelihood of detection, we used regenerating
166 scales, in which the scleroblasts were activated and were therefore larger compared with those in ontogenetic
167 scales [11]. Individuals were anesthetized in a solution of 0.1% 2-phenoxyethanol and 30 scales were removed
168 from the left flank. The lateral line scales were not used. After 7 days, the skin containing the regenerating scales
169 was dissected and fixed in 10% formalin solution for overnight at 4°C. After fixation, the samples were
170 decalcified in Morse's solution (10% sodium citrate and 22.5% formic acid) [12] for 1 day at 4°C. The samples
171 were then dehydrated conventionally, embedded in TissuePrep (Fisher Scientific, Fair Lawn, NJ, USA), and
172 sections (6 µm) were cut frontally. After deparaffinization and rehydration, the sections were treated with 1.0
173 µg/ml proteinase K in phosphate buffered saline (pH 7.4) for 15 min at 37°C, and were hybridized with the
174 probes at 42°C overnight. The sections were washed twice with 2×SSC and then twice with 0.1×SSC at 50°C for
175 30 min. The signal was visualized with alkaline phosphatase-conjugated anti-digoxigenin antibody (Roche) and
176 nitro blue tetrazolium/5-bromo-4-chloro-3-indolyl-phosphate solution (Roche).

177

178 **Results**

179

180 Identification of proteins by tandem mass spectrometry

181

182 More than 100 spots were detected by 2-DE with molecular weights of 100–10 kDa (Fig. 1). The acidic spots,
183 having molecular weights of 75–37 kDa and less than 20 kDa, were smeared. Clear spots with molecular weights
184 of 35–25 kDa were observed in the neutral region. A number of clear spots were observed in the alkaline region
185 with molecular weights of 75–10 kDa.

186 We excised 25 spots from the 2-DE gel for MS/MS analysis, but succeeded to identify only three
187 proteins: dermatopontin, lysyl oxidase, and biglycan (spots #1, 2, and 3 in Fig. 1), as described below.

188 In a Mascot search [10] for spot #1, the amino acid sequences of two peptides,

189 (R)QGFNFQCPHGEVLVAVR(S) and (K)YFEAVLDREWQFYCCR(Y), matched that of zebrafish

190 dermatopontin (GenBank accession no. NM_001030085). In a Mascot search for spot #2, the amino acid

191 sequences of two peptides, (K)NQGTADFLPSRPR(Y) and (R)VKNQGTADFLPSRPR(Y), matched that of
192 Atlantic salmon *Salmo salar* lysyl oxidase (GenBank accession no. DQ167812). Similarly, from spot #3, the
193 amino acid sequences of three peptides, (R)HIEHGALSYLTLNR(E), (K)VFYNGISLFDNPIR(Y), and
194 (R)YWEVQPSTFR(C), matched that of zebrafish biglycan (GenBank accession no. NM_001002227).

195

196 cDNA cloning and mRNA expression analyses of goldfish dermatopontin

197

198 Dermatopontin is closely linked to collagen fibrillogenesis as well as organization of collagen fibrils in
199 mammals [9, 13, 14]. Additionally, at the time we initiated this study, knowledge of fish dermatopontin was
200 limited to a single zebrafish dermatopontin gene on the database, which was predicted to yield a protein.
201 Therefore, we targeted dermatopontin for further analysis and conducted cDNA cloning.

202 The cloned goldfish dermatopontin cDNA had 1074 bp (DDBJ, accession no. AB576186) and
203 contained an open reading frame encoding 196 amino acids. The alignments of an amino acid sequence predicted
204 from goldfish dermatopontin cDNA (obtained in this study) with the sequences of zebrafish, *Xenopus laevis*,
205 chicken *Gallus gallus domesticus*, and human *Homo sapiens* (obtained from databases) is given in Figure 2. Data
206 for zebrafish dermatopontin from cloned cDNA, which was uploaded from our laboratory during this study [15],
207 was used in Fig. 2. The two amino acid sequences matched with zebrafish dermatopontin by MS/MS analysis
208 were found in the obtained goldfish sequence (Fig. 2). However, one valine in the zebrafish sequence
209 (QGFNFQCPHGEVLVAVR) was substituted with isoleucine (QGFNFQCPHGEVLVAIR) in goldfish. The
210 predicted molecular weight of goldfish dermatopontin, excluding signal peptides (21 amino acids inferred by
211 SignalP 3.0 Server; <http://www.cbs.dtu.dk/services/SignalP-3.0/>), was 21.0 kDa.

212 The amino acid sequence of goldfish dermatopontin had 88% homology with that of zebrafish, 62%
213 with *Xenopus*, 57% with chicken, and 56% with human. All 10 cysteine residues observed in mammalian
214 dermatopontin were conserved in goldfish dermatopontin.

215 Mammalian dermatopontins have three characteristic motifs [16, 17]. The first is a sequence of six
216 amino acids, DRE/QWXF/Y (where X is any amino acid). Similar sequences at appropriate sites were all
217 conserved in goldfish dermatopontin (Fig. 2). The second and the third motifs are the integrin-binding RGAT
218 sequence and a consensus sequence NYD that is observed in many amine oxidases. However, these motifs were
219 not conserved in either goldfish or zebrafish dermatopontin (Fig. 2).

220 RT-PCR analysis revealed that dermatopontin was expressed in all the tissues examined in this study
221 (Fig. 3).

222 The frontal sections of goldfish skin that contained 7-day regenerating scales are illustrated in Figure 4.
223 Three-types of scale-forming scleroblasts, flat episquamal, square hyposquamal, and oval- to droplet-shaped
224 marginal scleroblasts, were attached on the scale matrix (Fig. 4A). *In situ* hybridization revealed that
225 dermatopontin mRNA was primarily expressed in the hyposquamal scleroblasts (Fig. 4B). No positive reaction
226 was detected when the sense probe was used (data not shown).

227

228 **Discussion**

229

230 This is the first study to apply MS/MS analysis to identify NCPs contained in teleost fish scales. Although the
231 identification efficiency was low, a protein having an apparent molecular weight of 19-kDa was identified as
232 dermatopontin. Dermatopontin, formerly known as tyrosine-rich acidic matrix protein (TRAMP) [18], was first
233 purified from bovine skin [19]. It is an acidic protein (isoelectric point: ca. 4.2) composed of 183 amino acids
234 with an apparent molecular weight on SDS-PAGE of 22 kDa. Its N-terminal region is rich in tyrosine residues,
235 and many of them are sulphated [18, 20]. The apparent molecular weight and isoelectric point (ca 5.0) of the
236 goldfish dermatopontin identified in our study largely agreed with those of bovine dermatopontin. Additionally,
237 we cloned and sequenced a dermatopontin homolog from the cDNA of goldfish scales, and found that it had 175
238 amino acids in the mature form (predicted molecular weight: 21 kDa). Thus, the apparent molecular weight of
239 goldfish dermatopontin on the SDS-PAGE (19 kDa) was smaller, but its reason is presently unknown.

240 Purification and amino acid sequence analysis of the protein will further clarify matured form of dermatopontin
241 in goldfish tissues. The deduced amino acid sequence also revealed that all 10 cysteine residues conserved
242 among mammalian dermatopontins were also conserved in goldfish dermatopontin, suggesting that it shares a
243 similar three-dimensional conformation to mammalian dermatopontins. Mammalian dermatopontins have five
244 loop structures composed of five intramolecular disulfide bonds [16].

245 Dermatopontin is closely linked to collagen fibrillogenesis and organization of collagen fibrils in
246 mammals. Dermatopontin purified from porcine skin accelerated type I collagen fibrillogenesis *in vitro*, and the
247 synthesized fibrils were relatively thin and had a narrower range of diameters in the presence of dermatopontin
248 [13]. Dermatopontin-null mice exhibited decreased thickness of the dermis, a lower skin collagen content, and
249 had larger diameter collagen fibrils with irregular contours [14]. The range of collagen fibril diameters in the

250 dermis of dermatopontin-null mice was also greater. Moreover, Cooper et al. [9] reported that the corneal stroma
251 of dermatopontin-null mice had larger collagen-fibril spacing and disrupted fibrillar organization. Because the
252 expression of goldfish dermatopontin mRNA in the regenerating scales was primarily detected in the
253 hyposquamal scleroblasts responsible for the production of the basal plate, the data obtained in mammals to date
254 strongly suggest that dermatopontin regulates collagen fibrillogenesis and formation of the cornea-like
255 plywood-like collagen-fibril assembly of the basal plate. However, there remains a need for further analysis on
256 the function of dermatopontin during collagen assembly in the basal plate.

257 Our results also demonstrate that goldfish dermatopontin mRNA expression is not specific to scales.
258 We detected a positive signal in a wide range of tissues, including the skin, fin, eye, skeletal muscle, heart, brain,
259 kidney, liver, swim bladder, and blood cells. Dermatopontin in mammals and zebrafish is also distributed in a
260 wide range of tissues [15, 16, 20, 21], suggesting that it has multiple functions. Two functions of dermatopontin,
261 other than regulating collagen fibrillogenesis, have been proposed [16]. These include promotion of cell
262 adhesion and fine tuning of activity of TGF- β , a cytokine playing a central role in wound healing of skin [22].
263 Recent research suggests that dermatopontin promotes epidermal keratinocyte adhesion via $\alpha 3\beta 1$ integrin and a
264 proteoglycan receptor (likely to be syndecan) [23]. Although the recognition sequence of $\alpha 3\beta 1$ integrin in
265 dermatopontin was not clarified, the binding site of the proteoglycan receptor was identified as an eight amino
266 acid sequence, GQVVAVR [23]. A similar sequence was also observed in goldfish and zebrafish
267 dermatopontins, but substitutions of some amino acids were observed [GEVLVAIR (goldfish residues 48–55)
268 and GEVLVAVR (zebrafish residues 35–42), Fig. 2]. Moreover, the predicted integrin-binding site sequence
269 (RGAT) conserved in mammalian dermatopontins was not conserved in goldfish and zebrafish (Fig. 2). Thus,
270 the cell-adhesion activity of dermatopontin should be studied carefully in fish.

271 Our MS/MS analysis also identified lysyl oxidase and biglycan. Lysyl oxidase is an enzyme secreted
272 into the ECM, which oxidizes lysine residues in collagen and initiates formation of covalent cross-linkages that
273 stabilize collagen fibrils [24, 25]. Thus, lysyl oxidase activity is closely related to the strength of the fibrils and,
274 hence, of the tissue. Lysyl oxidase in goldfish scale basal plates may also increase the strength of the plates by
275 promoting cross-linking of collagen fibrils. Biglycan is a member of the Class I small leucine-rich proteoglycans
276 (SLRPs) [26]. In tendon tissue, biglycan-null mice exhibit a decrease in the number of fibrils with a larger
277 diameter, and an increase in those with a smaller diameter [27]. However, unusually large fibrils also occur in
278 these mice. In cornea tissue, biglycan has a supportive role for decorin, another class I SLRP that regulates
279 collagen fibrillogenesis in this tissue. Double knock-out mice lacking both decorin and biglycan exhibit

280 abnormally thick collagen fibrils with an irregular contour, and disruption in fibril packing and lamellar
281 organization [28]. However, single knockout mice lacking either decorin or biglycan do not exhibit significant
282 changes in corneal collagen fibrils [28]. A compensatory up-regulation of biglycan gene expression was
283 observed in decorin-deficient mice, but not the reverse, suggesting that decorin plays a primary role in regulating
284 fibril assembly in the cornea, and that biglycan fine-tunes the function of decorin [28]. Although decorin was not
285 detected in this study, it is possible that biglycan with decorin has an important role in the regulation of collagen
286 fibrillogenesis in the scale basal plate of goldfish.

287 Aiming to obtain collagen-associated NCPs from the scale basal plate, the present study employed a
288 0.5 M acetic acid solution as an extraction solution, because the acidic solution is usually used to extract
289 collagen molecules. However, more broader spectrum of proteins in the basal-plate matrix seem to be contained
290 in the extract, because many spots were obtained by 2DE analysis. On the other hand, the present extraction
291 method may also be an incomplete one, because a large part of basal plate matrix was discarded as a precipitates
292 of the extraction in this study. Protein denaturation agents such as urea, guanidine-HCl or CHAPS may be
293 contained in the solution to extract proteins from the precipitates. In fact, Jiang et al. [29] showed a need of
294 sequential extraction of dog bone for complete proteome analysis. They sequentially used a 1.2 M HCl solution,
295 a 100 mM Tris buffer (pH 7.4) solution with 6 M guanidine-HCl, the same buffer solution containing 6 M
296 guanidine-HCl and 0.5 M tetrasodium EDTA, and a 6 M HCl solution for extraction. They reported that only
297 0.77 mg protein out of 3.77 mg of total proteins obtained by the sequential extraction was extracted by the first
298 acid extraction. However, the acid extract contained most of the bone-specific matrix proteins, suggesting the
299 acid extraction is the efficient method for the purpose of the present study.

300 Zebrafish is the most frequently used model teleost in the recent biomedical research [30], but we used
301 goldfish scales to identify NCPs of the basal plate in the present study. This is because goldfish is much bigger
302 in body and scale size than zebrafish. The bigger scale size makes to collect basal plate samples much easier.
303 The bigger body size may also beneficial in future. It may be possible to purify both collagen and dermatopontin
304 from goldfish, and conduct *in vitro* fibrillogenesis experiments to clarify function of goldfish dermatopontin. In
305 porcine, dermatopontin was reported to accelerate collagen fibrillogenesis, and the produced fibrils in the
306 presence of dermatopontin became thinner than its absence [13]. Another beneficial point to use goldfish is that
307 goldfish and zebrafish are included in the same family Cyprinidae; thus, zebrafish genome data can be applied, at
308 least in part, when MS/MS analysis is performed. In fact, the peptides from two identified proteins matched that

309 of zebrafish data in the present MS/MS analysis. The PCR primers designed based on zebrafish dermatopontin
310 also worked well. Therefore, we believe that gold fish is a suitable species for the purpose of the present study.

311

312 **Acknowledgments**

313

314 This work was supported in part by Grants in Aid from the Japanese Ministry of Education, Culture, Sports,
315 Science and Technology (Nos. 18380109, 21380116, 24380101).

316

317 **References**

318

- 319 1. Takagi Y, Ura K (2007) Teleost fish scales: a unique biological model for the fabrication of materials for
320 corneal stroma regeneration. *J Nanosci Nanotech* 7:757-762
- 321 2. Schnaper HW, Kleinman HK (1993) Regulation of cell function by extracellular matrix. *Pediatr Nephrol*
322 7:96-104
- 323 3. Streuli C (1999) Extracellular matrix remodelling and cellular differentiation. *Curr Opin Cell Biol*
324 11:634-640
- 325 4. Kresse H, Schönherr E (2001) Proteoglycans of the extracellular matrix and growth control. *J Cell Physiol*
326 189:266-274
- 327 5. Marastoni S, Ligresti G, Lorenzon E, Colombati A, Mongiat M (2008) Extracellular matrix: a matter of life
328 and death. *Connect Tissue Res* 49:203-206
- 329 6. Parenteau-Bareil R, Gauvin R, Berthod F (2010) Collagen-based biomaterials for tissue engineering
330 applications. *Materials* 3:1863-1887
- 331 7. Yamada S, Yamamoto K, Ikeda T, Yanagiguchi K, Hayashi Y (2014) Potency of fish collagen as a scaffold
332 for regenerative medicine. *BioMed Res Int* 2014, Article ID 302932, 8 pages,
333 <http://dx.doi.org/10.1155/2014/302932>
- 334 8. Parfitt GJ, Pinali C, Young RD, Quantock AJ, Knupp C (2010) Three-dimensional reconstruction of
335 collagen-proteoglycan interactions in the mouse corneal stroma by electron tomography. *J Struct Biol*
336 170:392-397

- 337 9. Cooper LJ, Bentley AJ, Nieduszynski IA, Talabani S, Thomson A, Utani A, Shinkai H, Fullwood NJ,
338 Beown GM (2006) The role of dermatopontin in the stromal organization of the cornea. *Invest Ophthalmol*
339 *Visual Sci* 47:3303-3310
- 340 10. Perkins DN, Pappin DJ, Creasy DM, Cottrell JS (1999) Probability-based protein identification by
341 searching sequence databases using mass spectrometry data. *Electrophoresis* 20:3551-3567
- 342 11. Ohira Y, Shimizu M, Ura K, Takagi Y (2007) Scale regeneration and calcification in the goldfish *Carassius*
343 *auratus*: quantitative and morphological process. *Fish Sci* 73:46-54
- 344 12. Morse A (1945) Formic acid-sodium citrate decalcification and butyl alcohol dehydration of teeth and
345 bones for sectioning in paraffin. *J Dental Res* 24:143-153
- 346 13. MacBeath JRE, Shackleton DR, Hulmes DJS (1993) Tyrosine-rich acidic matrix protein (TRAMP)
347 accelerates collagen fibril formation *in vitro*. *J Biol Chem* 268:19826-19832
- 348 14. Takeda U, Utani A, Wu J, Adachi E, Koseki H, Taniguchi M, Matsumoto T, Ohashi T, Sato M, Shinkai H
349 (2002) Targeted disruption of dermatopontin causes abnormal collagen fibrillogenesis. *J Invest Dermatol*
350 119:678-683
- 351 15. Tan Y, Iimura K, Sato T, Ura K, Takagi Y (2013) Spatiotemporal expression of the dermatopontin gene in
352 zebrafish *Danio rerio*. *Gene* 516:277-284
- 353 16. Okamoto O, Fujiwara S (2006) Dermatopontin, a novel player in the biology of the extracellular matrix.
354 *Connect Tissue Res* 47:177-189
- 355 17. Takeuchi T (2010) Structural comparison of dermatopontin amino acid sequences. *Biologia* 65:874-879
- 356 18. Cronshaw AD, Macbeath JRE, Shackleton DR, Collins JF, Fothergill-Gilmore LA, Hulmes DJS (1993)
357 TRAMP (Tyrosine Rich Acidic Matrix Protein), a protein that co-purifies with lysil oxidase from porcine
358 skin: identification of TRAMP as the dermatan sulphate proteoglycan-associated 22K extracellular matrix
359 protein. *Matrix* 13:255-256
- 360 19. Neame PJ, Choi HU, Rosenberg LC (1989) The isolation and primary structure of a 22-kDa extracellular
361 matrix protein from bovine skin. *J Biol Chem* 264:5474-5479
- 362 20. Forbes EG, Cronshaw AD, MacBeath JRE, Hulmes DJS (1994) Tyrosine-rich acidic matrix protein
363 (TRAMP) is a tyrosine-sulphated and widely distributed protein of the extracellular matrix. *FEBS Lett*
364 351:433-436

- 365 21. Superti-Furga A, Rocchi M, Schäfer BW, Gitzelmann R (1993) Complementary DNA sequence and
366 chromosomal mapping of a human proteoglycan-binding cell-adhesion protein (dermatopontin). *Genomics*
367 17: 463-467
- 368 22. Beanes SR, Dangng C, Soo C, Ting K (2003) Skin repair and scar formation: the central role for TGF- β . *Exp*
369 *Rev Mol Med* 5:1-11
- 370 23. Okamoto O, Hozumi K, Katagiri F, Takahashi N, Sumiyoshi H, Matsuo N, Yoshioka H, Nomizu M,
371 Fujiwara S (2010) Dermatopontin promotes epidermal keratinocyte adhesion via $\alpha 3\beta 1$ integrin and a
372 proteoglycan receptor. *Biochemistry* 49:145-155
- 373 24. Kagan MH, Li W (2003) Lysyl oxidase: properties, specificity, and biological roles inside and outside of
374 the cell. *J Cell Biochem* 88:660-672
- 375 25. Trackman CP (2005) Diverse biological functions of extracellular collagen processing enzymes. *J Cell*
376 *Biochem* 96:927-937
- 377 26. Schaefer L, Iozzo R (2008) Biological functions of the small leucine-rich proteoglycans: from genetics to
378 signal transduction. *J Biol Chem* 283:21305-21309
- 379 27. Corsi A, Xu T, Chen X-D, Boyde A, Liang J, Mankani M, Sommer B, Iozzo RV, Eichstetter I, Gheron
380 Robey P, Bianco P, Young MF (2002) Phenotypic effects of biglycan deficiency are linked to collagen
381 fibril abnormalities, are synergized by decorin deficiency, and mimic Ehlers-Danlos-like changes in bone
382 and other connective tissues. *J Bone Min Res* 17:1180-1189
- 383 28. Zhang G, Chen S, Goldoni S, Calder B, Simpson H, Owens R, McQuillan D, Young M, Iozzo R, Birk D
384 (2009) Genetic evidence for the coordinated regulation of collagen fibrillogenesis in the cornea by decorin
385 and biglycan. *J Biol Chem* 284:8888-8897
- 386 29. Jiang X, Ye M, JIang X, Liu G, Feng S, Cui L, Zou H (2007) Method development of efficient protein
387 extraction in bone tissue for proteome analysis. *J Proteome Res* 6:2287-2294
- 388 30. Brittijn SA, Brittijn A, Duivesteijn SJ, Belmamoune M, Bertens LFM, Bitter W, De Bruijin J, Champagne
389 DL, Cuppen E, Flik G, Vandenbroucke-Grauls CM, Janssen RAJ, De Jjong IML, De Kloet ER, Kros A,
390 Meijer AH, Mets JR, Van Der Sar AM, Schaaf MJM, Schlute-Merker S, Spainkll HP, Tak PP, Vereek FJ,
391 Vervoordeldonk MJ, Vonk FJ, Witte F, Yuan H, Richardson M (2009) Zebrafish development and
392 regeneration: new tools for biomedical research. *Int J Dev Biol* 53:835-850

393

394

395 **Figure captions**

396

397 **Fig. 1** Two-dimensional gel electrophoresis profile of an acetic acid extract from the basal plates of goldfish
398 *Carassius auratus* scales. The gel was stained with silver. *Dotted circle* spots identified by MS/MS analysis, *M*
399 marker, *pI* isoelectric point

400

401 **Fig. 2** Alignments of amino acid sequences of dermatopontin of goldfish, zebrafish, *Xenopus*, chicken and
402 human. *Black box* sequences matched with zebrafish dermatopontin by MS/MS analysis, *open box* sequences of
403 six amino acids D-R-E/Q-W-X-F/Y (where X is any amino acid), *dotted box* cysteine residues, *underline*
404 integrin-binding R-G-A-T sequences, *dotted underline* N-Y-D sequences, *asterisk* conserved amino acids, *dot*
405 *symbol* amino acid similarity

406

407 **Fig. 3** Tissue distribution of goldfish dermatopontin mRNA expression based on RT-PCR. *M* marker, *Sc* scale,
408 *Sk* skin, *Fi* caudal fin, *Ey* eye, *Ms* skeletal muscle, *He* heart, *Br* brain, *Ki* kidney, *Li* liver, *Sb* swim bladder, *Bc*
409 blood cells

410

411 **Fig. 4** *In situ* hybridization analysis of goldfish dermatopontin mRNA expression in a 7-day regenerated scale.
412 **a** Hematoxylin and eosin stained section; **b** antisense-probe reacted *in situ* hybridization section. *E* epithelium,
413 *ESb* episquamal scleroblasts, *HSb* hyposquamal scleroblasts, *MSb* marginal scleroblasts, *S* scale. *Bar* 50 μ m

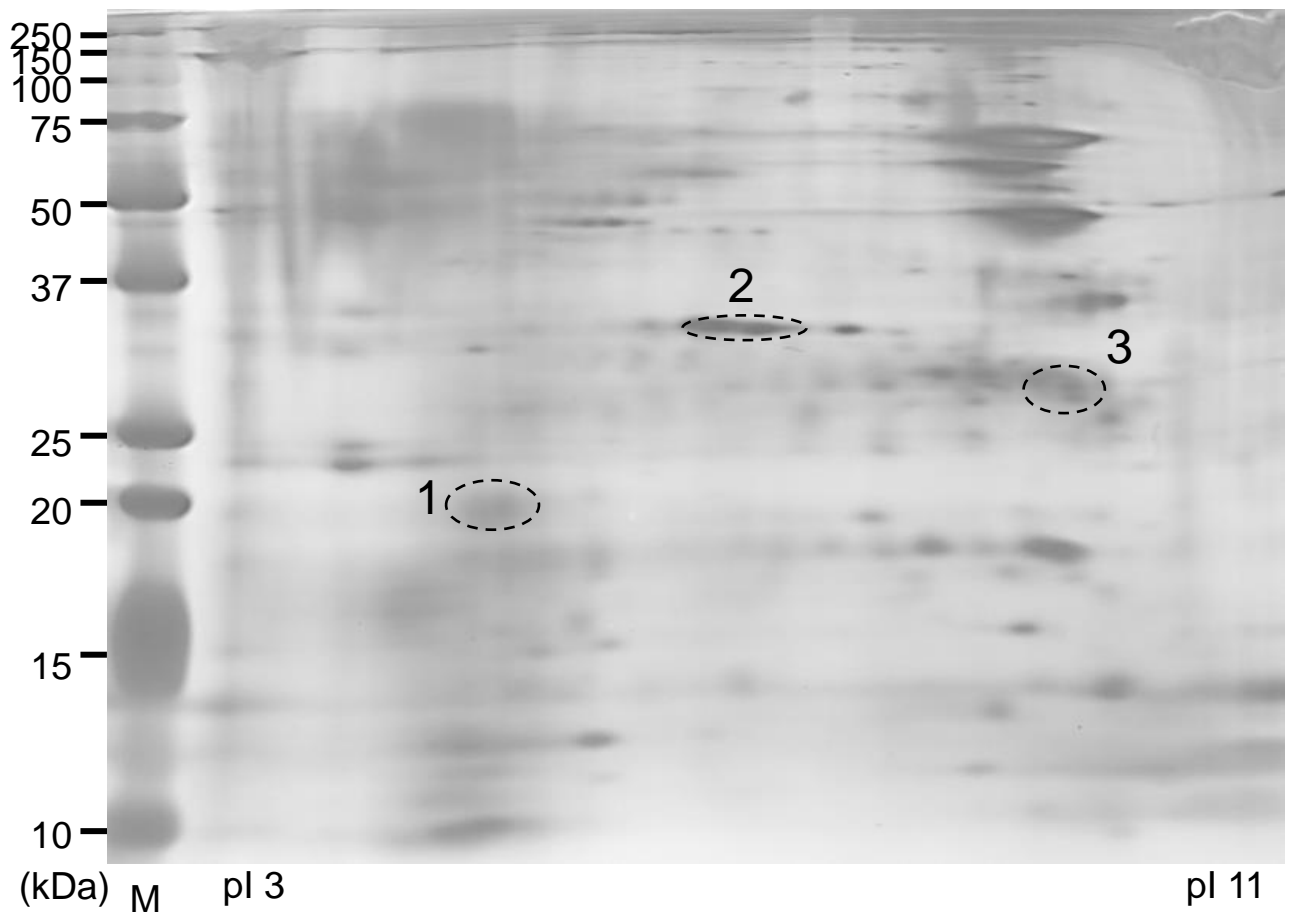


Fig.1
Komatsu et al.

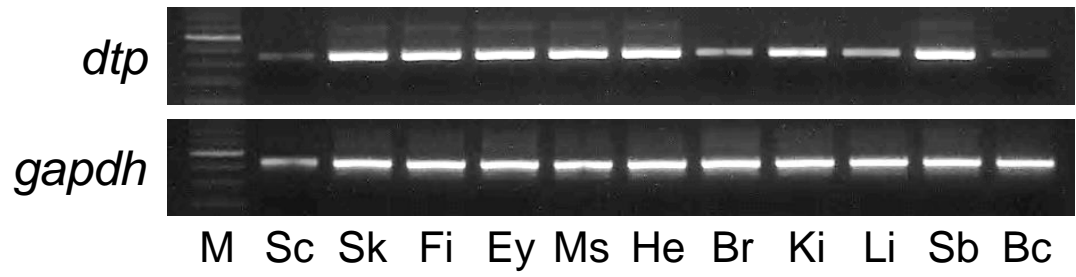


Fig. 3
Komatsu et al.

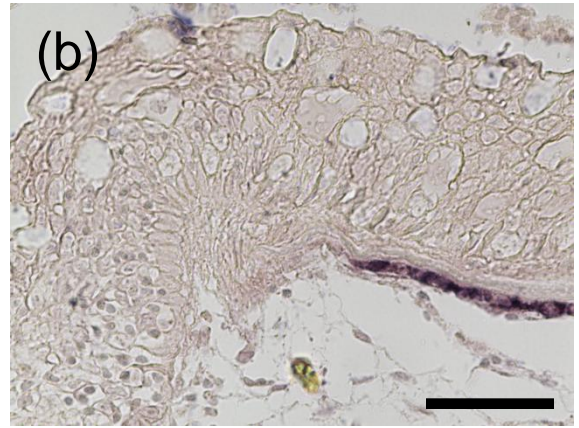
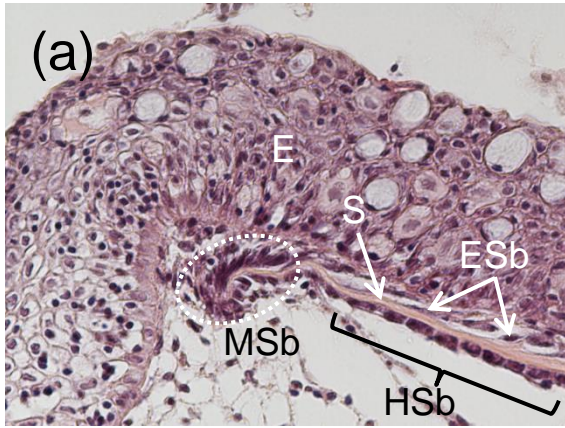


Fig. 4
Komatsu et al.